

PHOTOCATALYTIC DEGRADATION MECHANISM OF MALACHITE GREEN DYE USING Cu^{2+} DOPED TIN OXIDE-ZINC OXIDE NANOCOMPOSITES

K.J.Abhirama* & K.U.Madhu *

*Physics Research Centre, S.T.Hindu College, Nagercoil– 629002,
(Affiliated to Manonmaniam Sundaranar University, Tirunelveli) Tamil Nadu, India

Received: January 29, 2019

Accepted: March 18, 2019

ABSTRACT: The photocatalytic degradation mechanism of malachite green dye was carried out using Cu^{2+} doped $(\text{SnO}_2)_{1-x}(\text{ZnO})_x$ nanocomposites (with x values 0.0, 0.2, 0.4, 0.5, 0.6, 0.8 and 1.0) synthesized via simple microwave assisted solvothermal technique using a simple domestic microwave oven. The as-prepared samples were calcinated at 500 °C and the calcinated samples were used for observing the degradation of malachite green dye at different intervals of time under UV light irradiation. The degradation efficiency of Cu^{2+} doped tin oxide-zinc oxide nanocomposite with respect to irradiation time was calculated. Decrease in degradation efficiency was observed for doped $(\text{SnO}_2)_{1-x}(\text{ZnO})_x$ nanocomposites when compared to undoped $(\text{SnO}_2)_{1-x}(\text{ZnO})_x$ nanocomposites. The result obtained were discussed and reported.

Key Words: Catalyst, malachite green, photocatalytic degradation, solvothermal, UV irradiation.

Highlights: Photocatalytic degradation mechanism of malachite green dye was carried out using the prepared nanocomposites.

1.Introduction:

Discharge of hazardous industrial wastes into the water bodies and air resulted in serious environmental issues [1]. Hence it is necessary to remove these hazardous substances before discharging it into the environment. The toxic substances generated from dyes can be removed through physical and chemical processes such as precipitation, flocculation, adsorption, ultra-filtration, reverse osmosis and advanced oxidation processes [2]. Photocatalysis emerges as an efficient method for the purification of water [3, 4]. In the photocatalytic process, electron-hole pairs are generated by means of band-gap radiation, which in turn give rise to redox reactions with the species adsorbed on the surface of the photocatalyst [5]. Photocatalysis is used as a pre-treating unit for the degradation of non-biodegradable organic pollutant to biodegradable compounds possessing low molecular weight [6]. Coupling of semiconductor photocatalyst results in higher photocatalytic efficiency thereby increasing the charge separation and extending the energy range of photoexcitation [7].

Malachite green dye is a triphenylmethane dye used as fungicide in aqua culture [8]. It is used in paper industry [9], textile industry for dyeing silks [10]. It is a cationic dye and it is soluble in water [11]. It is toxic and it causes diseases such as carcinogenesis, mutagenesis, chromosomal fractures, teratogenicity and respiratory toxicity [12]. Jayant et al [13] reported the photocatalytic bleaching of malachite green and brilliant green dyes using ZnS- CdS photocatalyst. Sudhaparimala et al [14] reported the photocatalytic degradation of methyl orange dye using SnO_2 -ZnO nanocomposite. In the present work the degradation of malachite green dye under UV light irradiation was carried out using Cu^{2+} doped tin oxide- zinc oxide nanocomposites prepared by a simple microwave assisted solvothermal technique as catalyst.

2.Experimental and Characterization:

Cu^{2+} doped $(\text{SnO}_2)_{1-x}(\text{ZnO})_x$ nanocomposites (with x values 0.0, 0.2, 0.4, 0.5, 0.6, 0.8 and 1.0) were synthesized using a simple microwave assisted solvothermal method and the experimental procedure was explained in detail in our earlier work [15]. The as prepared samples were calcinated at 500 °C for 1hr and the calcinated samples were used to carry the photocatalytic activity. In the present work the photocatalytic activity of Cu^{2+} doped samples was explained in detail. Here 50 ml of 10 ppm aqueous malachite green solution was taken in a 100 ml beaker. 100 mg of prepared nanocomposite powder was added and stirred well using a magnetic stirrer for about 10 min. The dye solution containing the dispersed nanocomposite powder was kept in dark for about half an hour for achieving adsorption-desorption equilibrium. Then the solution was kept under UV light and was irradiated upto 6 hours. After every one hour interval 5 ml of

malachite green solution was taken out and it was centrifuged to remove the catalyst. Then it was characterized by UV-Vis spectral analysis.

The photocatalytic application studies of Cu²⁺ doped (SnO₂)_{1-x}(ZnO)_x (with x values 0.0, 0.2, 0.4, 0.5, 0.6, 0.8 and 1.0) nanocomposites was observed using Systronics 2201 UV-Visible double beam spectrophotometer in the wavelength range 200 - 800 nm. By observing the degradation mechanism of malachite green dye under UV light irradiation the photocatalytic activities of Cu²⁺ doped (SnO₂)_{1-x}(ZnO)_x nanocomposites were evaluated. For UV irradiation 18 W UV-AB fluorescent lamp was used. From the UV-Vis absorption spectra of malachite green solution the degradation of malachite green could be observed. The degradation efficiency was calculated using the formula [16, 17]. $D = \frac{100 * (C_i - C_e)}{C_i}$, where D is the degradation efficiency, C_i is the initial dye concentration and C_e is the dye concentration at definite interval of time.

3.Result and discussion:

The UV-Vis absorption spectra of malachite green dye at different intervals of time under the UV light irradiation observed for Cu²⁺ doped (SnO₂)_{1-x}(ZnO)_x nanocomposites are shown in Figures 1 - 7. Absorption in dark and photocatalysis under light illumination are the two phases occurring in the degradation process [18]. In oxide semiconductors electron-hole pairs was formed when the incident photons having energies greater than the band gap energy of the semiconductor transfer electron from valence band to the conduction band. The holes in the valence band are capable to generate hydroxyl radicals at the surface and they react with adsorbed dye molecules while the electron in the conduction band has the ability to reduce the oxygen molecules present in the solution. The hydroxyl radical thus formed is strong enough to carry out the degradation process [19]. Crystallite sizes play an important role in the photocatalytic activity. Large crystallite size particles possess small surface area which in turn low down the photocatalytic activity. The parameters such as pH of the reaction mixture, concentration of dye, light intensity, calcination temperature, photocatalyst load, initial concentration of dye, capping ligand and amount of semiconductor have direct impact on dye degradation [20-23]. Two different photooxidation pathways result in the decolorization of malachite green. They are: (i) the destruction of the chromophore structure and N-demethylation, and (ii) due to the formation of carbon-centered or nitrogen-centered radicals. Disappearances of colour of the dispersion specify that the chromophoric structure of the dye has been destroyed [24].

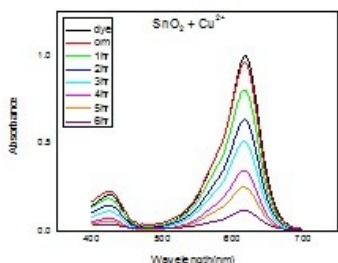


Figure 1: UV-Vis absorption spectra of malachite green dye at different intervals under UV light irradiation for SnO₂+ Cu²⁺ nanoparticles

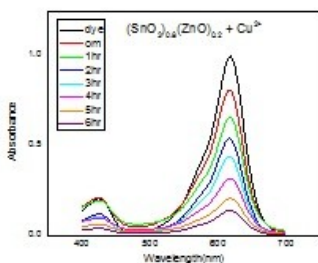


Figure 2: UV-Vis absorption spectra of malachite green dye at different intervals under UV light irradiation for (SnO₂)_{0.8}(ZnO)_{0.2}+ Cu²⁺ nanoparticles

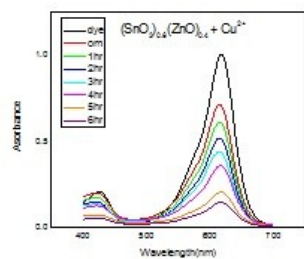


Figure 3: UV-Vis absorption spectra of malachite green dye at different intervals under UV light irradiation for (SnO₂)_{0.6}(ZnO)_{0.4}+ Cu²⁺ nanocomposite

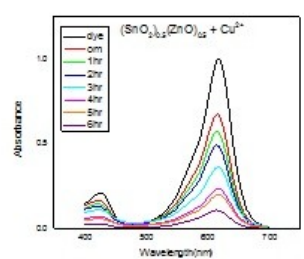


Figure 4: UV-Vis absorption spectra of malachite green dye at different intervals under UV light irradiation for (SnO₂)_{0.5}(ZnO)_{0.5}+ Cu²⁺ nanocomposite

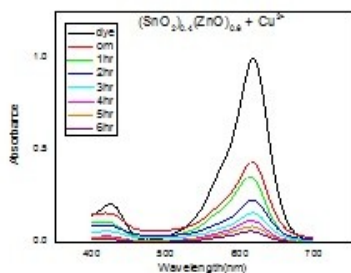


Figure 5: UV-Vis absorption spectra of malachite green dye at different intervals under UV light irradiation for $(\text{SnO}_2)_{0.4}(\text{ZnO})_{0.6} + \text{Cu}^{2+}$ nanocomposite

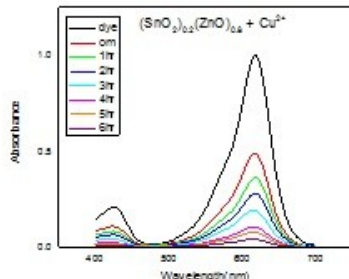


Figure 6: UV-Vis absorption spectra of malachite green dye at different intervals under UV light irradiation for $(\text{SnO}_2)_{0.2}(\text{ZnO})_{0.8} + \text{Cu}^{2+}$ nanocomposite

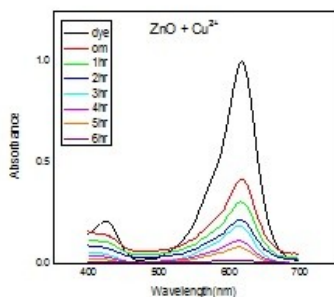


Figure 7: UV-Vis absorption spectra of malachite green dye at different intervals under UV light irradiation for $\text{ZnO} + \text{Cu}^{2+}$ nanoparticles

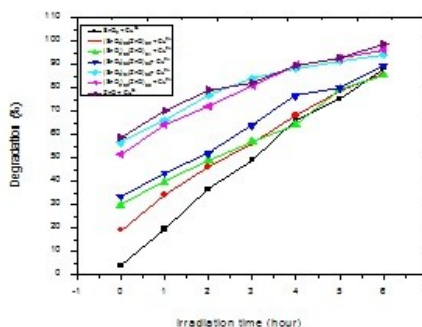


Figure 8: Degradation efficiency of Cu^{2+} doped $(\text{SnO}_2)_{1-x}(\text{ZnO})_x$ nanocomposites

The degradation efficiency of Cu^{2+} doped $(\text{SnO}_2)_{1-x}(\text{ZnO})_x$ nanocomposites with respect to irradiation time was shown in figure 8. It was observed that almost 55 % of degradation of dye occurs in solution containing Cu^{2+} doped ZnO as catalyst. This is because Cu^{2+} doped ZnO nanoparticles take part in degradation during the first phase. Cu^{2+} doped ZnO catalyst shows 90 % of degradation after an interval of 4 hrs. Cu^{2+} doped $(\text{SnO}_2)_{1-x}(\text{ZnO})_x$ (with x values 0.2, 0.4, 0.5, 0.6 and 0.8) nanocomposites shows lower activity when compared to Cu^{2+} doped ZnO. Similar to this result low photocatalytic activity of SnO_2 nanoparticles when compared to ZnO was reported by kowsari et al [25] and it was due to the difference in the surface area of the particles. In Cu^{2+} doped ZnO nanoparticles the recombinations of photogenerated electron-hole pairs are suppressed, hence it shows higher photocatalytic activity [26]. When compared to TiO_2 the band gap of ZnO is greater. So once excited, only few electrons fall back to the valence band, with a small energy loss and enhanced degradation efficiency [18].

It was observed that the degradation percentage decreases for Cu^{2+} doped $(\text{SnO}_2)_{1-x}(\text{ZnO})_x$ nanocomposites when compared to undoped $(\text{SnO}_2)_{1-x}(\text{ZnO})_x$ nanocomposites except Cu^{2+} doped ZnO. In Cu^{2+} doped ZnO percentage of degradation increases with the addition of dopant. This is because of the suppression of photogenerated electron-hole pair recombination. Also it has been observed that the percentage of degradation increases with increase in the concentration of ZnO. Degradation efficiency of Cu^{2+} doped $(\text{SnO}_2)_{1-x}(\text{ZnO})_x$ nanocomposites was shown in table 1. Decomposition ratio increases with degradation time [27].

Table 1: Degradation efficiency of Cu^{2+} doped $(\text{SnO}_2)_{1-x}(\text{ZnO})_x$ nanocomposites

System(with expected composition)	Degradation (%)
$\text{SnO}_2 + \text{Cu}^{2+}$	88
$(\text{SnO}_2)_{0.8}(\text{ZnO})_{0.2} + \text{Cu}^{2+}$	85
$(\text{SnO}_2)_{0.6}(\text{ZnO})_{0.4} + \text{Cu}^{2+}$	85
$(\text{SnO}_2)_{0.5}(\text{ZnO})_{0.5} + \text{Cu}^{2+}$	89

$(\text{SnO}_2)_{0.4}(\text{ZnO})_{0.6} + \text{Cu}^{2+}$	94
$(\text{SnO}_2)_{0.2}(\text{ZnO})_{0.8} + \text{Cu}^{2+}$	96
$\text{ZnO} + \text{Cu}^{2+}$	98

4. Conclusion

The degradation efficiencies of Cu^{2+} doped $(\text{SnO}_2)_{1-x}(\text{ZnO})_x$ nanocomposites was calculated and it was observed that almost 55 % of degradation of dye occurs in solution containing Cu^{2+} doped ZnO as catalyst. This is because Cu^{2+} doped ZnO nanoparticles take part in degradation during the first phase. Cu^{2+} doped $(\text{SnO}_2)_{1-x}(\text{ZnO})_x$ (with x values 0.2, 0.4, 0.5, 0.6 and 0.8) nanocomposites show lower photocatalytic activity when compared to Cu^{2+} doped ZnO. It was observed that the degradation percentage decreases for Cu^{2+} doped $(\text{SnO}_2)_{1-x}(\text{ZnO})_x$ nanocomposites when compared to undoped $(\text{SnO}_2)_{1-x}(\text{ZnO})_x$ nanocomposites except Cu^{2+} doped ZnO. In Cu^{2+} doped ZnO nanoparticles the recombinations of photogenerated electron-hole pairs are suppressed, hence it shows higher photocatalytic activity.

References

- HuihuWang, Seonghoon Baek, Jonghyuck Lee & Sangwoo Lim. Chemical Engineering Journal 2009; 146; 355–361.
- Manish Mittal, Manoj Sharma & O.P. Pandey. Solar Energy 2014; 110; 386–397.
- Chantal Guillard, Jean Disdier, Jean-Marie Herrmann, Corinne Lehaut, Thierry Chopin, Sixto Malato & Julian Blanco. Catalysis Today 1999; 54; 217–228.
- Maolin Zhang , Guoying Sheng, Jiamo Fu, Taicheng An, Xinming Wang & Xiaohong Hu. Materials Letters 2005; 59; 3641 – 3644.
- Cun Wang, Bo-Qing Xu, Xinming Wang & Jincal Zhao. Journal of Solid State Chemistry 2005; 178; 3500–3506.
- Gao Guandao, Zhang Aiyong, Zhang Meng, Chen Jinlong & Zhang Quanxing .Chinese Journal of Catalysis 2008; 29(5); 426–430.
- Zhaojie Wang, Zhenyu Li, Hongnan Zhang & Ce Wang. Catalysis Communications 2009; 11; 257–260.
- Daniel R. Doerge, Mona I. Churchwell, Theresa A. Gehring, Yu Ming Pu & Steven M. Plakas. Rapid Commun. Mass Spectrom 1998; 12; 1625–1634.
- Xueyan Liu, Shuai An, Wen Shi, Qi Yang & Lei Zhang. Journal of Molecular Catalysis A: Chemical 2014; vol. 395; 243–250.
- Yongming Ju, Shaogui Yang, Youchao Ding, Cheng Sun, Aiqian Zhang & Lianhong Wang. J. Phys. Chem. A 2008; vol. 112; 11172–11177.
- Zhongquan Wang & Yanmao Wen. Advanced Materials Research 2014; 838-841; 2745-2750.
- Atul Kumar Kushwaha, Neha Gupta & Chattopadhyaya MC. Journal of Saudi Chemical Society 2014; vol. 18; 200- 207.
- Jayant Gandhi, Rajesh Dangi, Jagdish Chandra Sharma, Nikhil Verma & Shipra Bhardwaj. Der Chemica Sinica 2010; 1 (3); 77-83.
- S. Sudhparimala & M. Vaishnavi. Materials Today: Proceedings 2016; 3; 2373–2380.
- Abhirama K.J & Madhu K.U. Int. Journal of Engineering Research and Application 2017; Vol.7, Issue 11, Part -7; 64-72.
- Xian-Jiao Zhou, Wan-Qian Guo, Shan-Shan Yang, He-Shan Zheng & Nan-Qi Ren. Bioresource Technology 2013; vol. 128; 827–830.
- Hadi Fallah Moafi, Abdollah Fallah Shojaie & Mohammad Ali Zanjanchi. Journal of Applied Polymer Science 2011; vol. 121; 3641–3650.
- Ramesh Raliya, Caroline Avery, Sampa Chakrabarti & Pratim Biswas. Appl Nanosci 2017; vol. 7; 253–259.
- Sajjad Khezrianjoo & Hosakere Doddarevanna Revanasiddappa. Journal of Catalysts 2013; 6 pages.
- Ameta, KL, Neema Papnai & Rakshit Ameta. Orbital: Electron. J. Chem 2014; vol. 6 (1); 14-19.
- Haydar Mohammad Salim. Journal of Environmental Science and Engineering A 2015; 4; 395-400.
- Xiaqing Chen, Zhansheng Wu, Dandan Liu & Zhenzhen Gao. Nanoscale Research Letters 2017; vol. 12; no. 143; 10 pages.
- Abebe Balcha, Om Prakash Yadav & Tania Dey. Environ Sci Pollut Res 2016; 9 pages.
- Zuoli He & Jiaqi Zhou. Modern Research in Catalysis 2013; vol. 2; 13-18.
- Elaheh Kowsari & Mohammad Reza Ghezelbash. Materials Letters 2012; 68; 17–20.
- Wang Cun, Zhao Jincal, Wang Xinming, Mai Bixian, Sheng Guoying, Peng Pingan & Fu Jiamo. Applied Catalysis B: Environmental 2002; 39; 269–279.
- Wenzhong Shen, Zhijie Li, Hui Wang, Yihong Liu, Qingjie Guo & Yuanli Zhang. Journal of Hazardous Materials 2008; 152; 172–175.